



## Article

# Long-Term Performance Evaluation of BeiDou PPP-B2b Products and Its Application in Time Service

Qianqian He <sup>1</sup>, Liang Chen <sup>2,\*</sup>, Lei Liu <sup>1</sup>, Daiyan Zhao <sup>1</sup>, Xiaopeng Gong <sup>3</sup> , Yidong Lou <sup>3</sup> and Qi Guan <sup>1</sup>

<sup>1</sup> China Electronics Technology Group Corporation No. 15th Research Institute, No. 211 Beisihuan Middle Road, Beijing 100083, China

<sup>2</sup> Beijing Institute of Tracking and Telecommunications Technology (BITTT), 26 Beiqing Road, Beijing 100094, China

<sup>3</sup> GNSS Research Center, Wuhan University, Luoyu Road 129, Wuhan 430079, China

\* Correspondence: chenliang@beidou.gov.cn

**Abstract:** Precise Point Positioning (PPP) is an official service of the BeiDou Global Navigation Satellite System (BDS-3) through the PPP-B2b signal. In this paper, we mainly focus on the long-term performance evaluation of BDS-3 PPP-B2b products and their application in time service. Since the PPP-B2b product is only available in and around China area, the arcs of PPP-B2b products are about several hours. We propose to evaluate the time datum stability by using all available satellites. Then, 557 day PPP-B2b products are collected for this experiment. The results show that there are large jumps in the GPS satellite clock time datum series. However, the BDS-3 satellite clock datum stability is almost at the same level with current Space State Representation (SSR) corrections from the International Global navigation satellite system Service (IGS). The difference between PPP-B2b GPS and BDS-3 satellite clock time datum will be absorbed into the Inter System Bias (ISB) parameter. Thus, it should be specially noted that the ISB parameter cannot be estimated as constant values if users use PPP-B2b products. In addition, the accuracy of the BDS-3 satellite clock is significantly better than that of the GPS for both the Root Mean Square Error (RMSE) and standard deviation (STD). The average Signal in Space Range Errors (SISREs) is 0.22 ns and 0.13 ns for GPS and BDS-3, respectively. The one-way timing experiment shows BDS-3 timing stability is  $2.9 \times 10^{-14}@10^4$  s. In addition, 10 baselines from 13 km to 4494 km are formed for time synchronization evaluation by using PPP-B2b products. The average RMSEs of time synchronization is from 0.46 ns to 1.58 ns and from 0.66 ns to 1.19 ns for GPS and BDS-3, respectively. As for STD, the average values are from 0.27 ns to 0.74 ns and from 0.27 ns to 0.47 ns for GPS and BDS-3, respectively. Overall, the results show that the time datum stability, accuracy, and service performance of BDS-3 PPP-B2b products has been stable over the past two years.

**Keywords:** BeiDou system; Precise Point Positioning; time synchronization



**Citation:** He, Q.; Chen, L.; Liu, L.; Zhao, D.; Gong, X.; Lou, Y.; Guan, Q. Long-Term Performance Evaluation of BeiDou PPP-B2b Products and Its Application in Time Service. *Remote Sens.* **2023**, *15*, 1358. <https://doi.org/10.3390/rs15051358>

Academic Editor: Giuseppe Casula

Received: 30 January 2023

Revised: 24 February 2023

Accepted: 24 February 2023

Published: 28 February 2023



**Copyright:** © 2023 by the authors. Licensee MDPI, Basel, Switzerland. This article is an open access article distributed under the terms and conditions of the Creative Commons Attribution (CC BY) license (<https://creativecommons.org/licenses/by/4.0/>).

## 1. Introduction

Positioning, Navigation, and Timing (PNT) are three core services of the Global Navigation Satellite System (GNSS) [1]. Compared with Real-Time Kinematic (RTK) technology, Precise Point Positioning (PPP) technology only needs one station for users to realize high-precision positioning and timing [2]. Thus, it is widely used for autopilot, space weather monitoring, and time and frequency transfer areas due to its high accuracy, flexibility, and proficiency [3–5]. However, PPP technology needs high-precision satellite orbit and clock products.

The BeiDou global navigation satellite system (BDS-3) is China's independently developed global navigation satellite system, which was completed on 31 July 2020 [6]. The BDS-3 provides six types of service, including PNT, satellite-based augmentation, PPP, regional short message communication, global short message communication, and international search and rescue [7]. Among them, the PPP service is available in China and

its surrounding areas based on satellite orbits, clocks, and differential code bias (DCB) corrections through the BDS-3 PPP-B2b signal [8–10].

Much research has focused on the evaluation of the accuracy and availability of BDS-3 PPP-B2b products. It was found that PPP-B2b corrections could greatly improve the discontinuous orbit and clock errors of broadcast ephemeris updating. In addition, the accuracy of the PPP-B2b orbit was slightly better than that of broadcast ephemeris, while the accuracy of the PPP-B2b clock improved by about 85% compared to that of broadcast ephemeris [11]. However, there are nonnegligible constant satellite-specific biases in the PPP-B2b clock offset for GPS and a smaller bias for BDS-3. One possible reason is the existence of signal distortion bias while the receiver types used for PPP-B2b and reference product calculation are different [12–14]. The Signal in Space Range Error (SISRE) of the PPP-B2b products is affected by this bias, but the SISRE standard deviation (STD) is at the same level as that of the CNES products [15,16]. The DCB parameters of PPP-B2b agree well with the parameters of the Multi GNSS Experiment (MGEX) DCB and time group delay (TGD) [17].

As for PPP performance, 7 day PPP results of BDS-3-only positioning using PPP-B2b products are in good agreement with the GPS-only results using CNES products. However, the average convergence time for GPS-only PPP using PPP-B2b products exceeds 60 min [15]. In addition, different PPP experiments are carried out using different observations, and the results show that centimeter-level and decimeter-level positioning accuracy can be obtained for static and dynamic situations, respectively [18–20]. Overall, the PPP performance based on PPP-B2b products is comparable to that of current International GNSS Service (IGS) Real Time Service (RTS) products [15] and can be further updated to PPP-RTK in the future [21]. Thus, it can be applied to coseismic displacement retrieval, urban environment navigation, ocean precise positioning, et al. [22–25]. As for time transfer, the difference of zero-baseline common clock difference (CCD) between PPP-B2b and GBM products is within 0.1 ns. However, the results of long-baseline time transfer between PPP-B2b and GBM products could reach up to 0.5 ns [26].

According to the above research, current research mainly analyzes the performance of PPP-B2b signal for positioning, and its application performance in time synchronization needs further investigation. In this contribution, we focus on the long-term performance of PPP time synchronization based on PPP-B2b signals. The paper is organized as follows: first, the models and methods used for PPP time synchronization are introduced. Then, the long-term characteristics of BDS-3 PPP-B2b orbit and clock corrections are analyzed with near 2 year data. Next, the performance of PPP time synchronization based on the PPP-B2b signal is presented. Finally, some conclusions are given.

## 2. Methods

### 2.1. Recovery and Evaluation of PPP-B2b Products

PPP-B2b products contain satellite orbit, clock, and code bias corrections, et al. Among them, the satellite orbit corrections are given in radial, along, and cross components. To recover precise satellite orbit in Earth-Centered, Earth-Fixed (ECEF) coordinate, the satellite orbit corrections should be first converted to ECEF coordinate:

$$\begin{pmatrix} \Delta_X \\ \Delta_Y \\ \Delta_Z \end{pmatrix} = (\mathbf{v}_R \quad \mathbf{v}_A \quad \mathbf{v}_C) \cdot \begin{pmatrix} \Delta_R \\ \Delta_A \\ \Delta_C \end{pmatrix} \quad (1)$$

$$\begin{cases} \mathbf{v}_R = \frac{\mathbf{r}}{|\mathbf{r}|} \\ \mathbf{v}_C = \frac{\mathbf{r} \times \dot{\mathbf{r}}}{|\mathbf{r} \times \dot{\mathbf{r}}|} \\ \mathbf{v}_A = \mathbf{v}_C \times \mathbf{v}_R \end{cases} \quad (2)$$

where  $(\Delta_R, \Delta_A, \Delta_C)$  is PPP-B2b satellite orbit corrections in radial, along, and cross components;  $(\Delta_X, \Delta_Y, \Delta_Z)$  represents satellite orbit corrections in ECEF coordinate converted from PPP-B2b corrections;  $\mathbf{r}$  is satellite position vector and  $\dot{\mathbf{r}}$  is satellite velocity vector;  $\mathbf{v}_R$ ,

$\mathbf{v}_C$ , and  $\mathbf{v}_A$  are the vectors used for orbit conversion. Then, precise satellite orbit and clock can be recovered:

$$\begin{cases} \begin{pmatrix} X_{B2b} \\ Y_{B2b} \\ Z_{B2b} \end{pmatrix} = \begin{pmatrix} X_{brdc} \\ Y_{brdc} \\ Z_{brdc} \end{pmatrix} - \begin{pmatrix} \Delta X \\ \Delta Y \\ \Delta Z \end{pmatrix} \\ t_{B2b}^s = t_{brdc}^s - \frac{\Delta_{clk}}{c} \end{cases} \quad (3)$$

where  $(X_{B2b}, Y_{B2b}, Z_{B2b})$  and  $t_{B2b}^s$  are the precise satellite orbit coordinate vector and clock offset recovered from PPP-B2b corrections;  $(X_{brdc}, Y_{brdc}, Z_{brdc})$  and  $t_{brdc}^s$  are the satellite orbit coordinate vector and clock of broadcaster ephemeris;  $\Delta_{clk}$  represents PPP-B2b satellite clock corrections;  $c$  denotes the speed of radio waves in vacuum.

In this paper, we mainly focus on the evaluation of product accuracy and time datum stability. To evaluate PPP-B2b satellite orbit and clock products, high-precision satellite orbit and clock products are chosen as reference products. First, we make a single difference between PPP-B2b products and reference products:

$$\begin{cases} \begin{pmatrix} \Delta X_{Dif} \\ \Delta Y_{Dif} \\ \Delta Z_{Dif} \end{pmatrix} = \begin{pmatrix} X_{B2b} \\ Y_{B2b} \\ Z_{B2b} \end{pmatrix} - \begin{pmatrix} X_{Ref} \\ Y_{Ref} \\ Z_{Ref} \end{pmatrix} \\ \Delta t_{Dif}^s = t_{B2b}^s - t_{Ref}^s \end{cases} \quad (4)$$

where  $(\Delta X_{Dif}, \Delta Y_{Dif}, \Delta Z_{Dif})$  and  $\Delta t_{Dif}^s$  are satellite orbit and clock differences between PPP-B2b products and reference products. Then, the satellite orbit vector  $(\Delta X_{Dif}, \Delta Y_{Dif}, \Delta Z_{Dif})$  can be converted to a satellite orbit vector in radial, along, and cross components  $(\Delta A_{Dif}, \Delta C_{Dif}, \Delta R_{Dif})$  according to Equation (1). Thus, the root mean square error (RMSE) of the satellite orbit can be calculated based on multi-epoch data. Different from the satellite orbit, satellite clocks from different organizations contain different time datum and can be expressed as follow:

$$t_*^s = t^s + T_* + \delta_*^s \quad (5)$$

where  $t_*^s$  is a specific satellite clock value and  $*$  represents a specific product, such as PPP-B2b;  $t^s$  is the true satellite clock;  $T_*$  is the time datum of a specific product;  $\delta_*^s$  is the error of the satellite clock. Thus, a single-differenced satellite clock between different products cannot eliminate the effect of clock time datum.

$$\Delta t_{Dif}^s = t_{B2b}^s - t_{Ref}^s = T_{B2b} - T_{Ref} + \delta_{B2b}^s - \delta_{Ref}^s \quad (6)$$

where  $\delta_{Ref}^s$  is the error of the reference satellite clock. Since the reference products are generally with high precision,  $\delta_{Ref}^s$  can be ignored. The clock time datum can be calculated by taking the average of all single-differenced satellite clocks:

$$\Delta T_{Dif} = \frac{1}{m} \sum_{s=1}^{s=m} \Delta t_{Dif}^s = T_{B2b} - T_{Ref} + \frac{1}{m} \sum_{s=1}^{s=m} \delta_{B2b}^s \quad (7)$$

where  $\frac{1}{m} \sum_{s=1}^{s=m} \delta_{B2b}^s$  is the average of PPP-B2b satellite clock errors. According to the results of [15], the PPP-B2b satellite clocks contain large biases. Thus, the term  $\frac{1}{m} \sum_{s=1}^{s=m} \delta_{B2b}^s$  will jump and affect the calculation of  $\Delta T_{Dif}$  if the available satellite number changes. Therefore, the satellite clock error  $\delta_{B2b}^s$  is divided into two parts:

$$\delta_{B2b}^s = \varepsilon_{ini}^s + \varepsilon_{B2b}^s \quad (8)$$

where  $\varepsilon_{ini}^s$  is the initial satellite clock error and is constant for each arc;  $\varepsilon_{B2b}^s$  is the satellite clock error except for the initial clock error. Thus, we propose to first remove the satellite initial error  $\varepsilon_{ini}^s$  for each arc. Then, we can get satellite clock time datum as follow:

$$\Delta T_{Dif} = T_{B2b} - T_{Ref} + \frac{1}{m} \sum_{s=1}^{s=m} \varepsilon_{B2b}^s \quad (9)$$

The clock time datum should be eliminated if we want to evaluate the RMSE and standard deviation (STD) of the satellite clock. We can get the double-differenced satellite clock by eliminating the time datum.

$$\Delta \nabla t_{Dif}^s = \Delta t_{Dif}^s - \Delta T_{Dif} = \delta_{B2b}^s - \frac{1}{m} \sum_{s=1}^{s=m} \varepsilon_{B2b}^s \quad (10)$$

where  $\Delta \nabla t_{Dif}^s$  is a double-differenced satellite clock error. Thus, the RMSE and STD of the satellite clock can be calculated based on multi-epoch  $\Delta \nabla t_{Dif}^s$ .

## 2.2. PPP Time Service

In GNSS time synchronization, ionospheric-free (IF) combination PPP is widely adopted since it eliminates the first order ionospheric delay. For simplicity, the noise terms are omitted, and the IF GNSS observations can be described as:

$$\begin{cases} P_{r,IF}^s = \rho + c \cdot (t_{r,sys} - t^s) + \alpha^s \cdot Trop \\ \Phi_{r,IF}^s = \rho + c \cdot (t_{r,sys} - t^s) + \alpha^s \cdot Trop + N_{IF} \end{cases} \quad (11)$$

where  $P_{r,IF}^s$  and  $\Phi_{r,IF}^s$  represent the IF pseudo-range and phase measurements from receiver  $r$  to satellite  $s$  ( $s = 1, 2, \dots, m$ ),  $m$  is the number of satellites tracked by receiver  $r$ ;  $\rho$  is the geometric distance with antenna phase center corrections;  $t_{r,sys}$  and  $t^s$  are the receiver and satellite clock error, respectively,  $sys$  denotes the satellite system of satellite  $s$ ;  $Trop$  is the zenith tropospheric delay that can be converted to slant with the mapping function  $\alpha^s$ ;  $N_{IF}$  is float ambiguity of phase observation. In IF PPP processing, the estimated parameters generally include receiver coordinate, receiver clock, zenith tropospheric delay, and ambiguity:

$$\begin{cases} E(l) = \mathbf{A} \cdot (\mathbf{X} \quad \bar{t}_r \quad Trop \quad \bar{\mathbf{N}}) \\ D(l) = \delta_0^2 \cdot \begin{pmatrix} \mathbf{U}_{2 \cdot m} \\ 10^{-4} \cdot \mathbf{U}_{2 \cdot m} \end{pmatrix} \end{cases} \quad (12)$$

$$l = \left( \tilde{P}_{r,IF}^1 \quad \tilde{P}_{r,IF}^2 \quad \dots \quad \tilde{P}_{r,IF}^m \quad \tilde{\Phi}_{r,IF}^1 \quad \tilde{\Phi}_{r,IF}^2 \quad \dots \quad \tilde{\Phi}_{r,IF}^m \right)^T \quad (13)$$

where  $\mathbf{X}$  is the receiver coordinate vector;  $\bar{t}_r$  is the receiver clock;  $\bar{\mathbf{N}}$  is the ambiguity vector;  $\mathbf{A}$  is the design matrix;  $\mathbf{U}_{2 \cdot m}$  is a  $2m \times 2m$  identity matrix; the value  $10^{-4}$  is determined since the weight of pseudo-range and phase is generally treated as 1:100;  $\tilde{P}_{r,IF}^m$  and  $\tilde{\Phi}_{r,IF}^m$  are the Observation-Minus-Calculation (OMC) values;  $\delta_0^2$  is the unit weight variance; Based on Equations (11)–(13), we can obtain float PPP solution by using square root information filter (SRIF) method. Since we focus on-time service, we mainly analyze the receiver clock parameter. In PPP processing, the satellite clock time datum will be absorbed by the receiver clock. Therefore, the estimated receiver clock is defined as follows:

$$\bar{t}_{r,sys} = t_{r,sys} + T_* + \sigma_{tr} \quad (14)$$

where  $\bar{t}_{r,sys}$  is the estimated receiver clock;  $t_{r,sys}$  is the true receiver clock;  $T_*$  is the time datum of the precise product used;  $\sigma_{tr}$  is the estimated receiver clock error. If we use a high-performance atomic receiver clock, the estimated receiver clock can also be used for precise product time datum stability evaluation. As for time synchronization, the time datum can be eliminated by the single difference between two stations:

$$\Delta \bar{t}_{r,sys} = \bar{t}_{r1,sys} - \bar{t}_{r2,sys} = t_{r1,sys} - t_{r2,sys} + \Delta \sigma_{tr} \quad (15)$$

where  $\Delta \bar{t}_{r,sys}$  is the single-differenced receiver clock;  $\Delta \sigma_{tr}$  is the single-differenced receiver clock error. To evaluate the performance of time synchronization, the single-differenced

receiver clock estimated by using post-processed satellite orbit and clock products is used as the reference value.

$$\Delta \nabla \bar{t}_{r,sys} = \Delta \bar{t}_{r,sys} - \Delta \hat{t}_{r,sys} = \Delta \sigma_{tr} - \Delta \varepsilon_{tr} \quad (16)$$

where  $\Delta \nabla \bar{t}_{r,sys}$  is the double-differenced receiver clock;  $\Delta \bar{t}_{r,sys}$  is the single-differenced receiver clock estimated by using post-processed satellite orbit and clock products;  $\Delta \varepsilon_{tr}$  is the single-differenced receiver clock error estimated by using post-processed satellite orbit and clock products and can generally be ignored.

### 3. Evaluation of PPP-B2b Products

In this section, the GPS and BDS-3 satellite orbit and clock accuracy of PPP-B2b products are evaluated. The time session is from Modified Julian Day Number (MJDN) 59,079 (18 August 2020) to 59,740 (11 June 2022). The PPP-B2b products are collected by our receivers. Due to some missing days of data, the actual valid time is 557 days. As for the reference products, we use the multi-system final satellite orbit and clock products from GeoForschungsZentrum (GFZ) and Wuhan University (WHU). The products of GFZ and WHU are namely gbm and wum, respectively. They can be downloaded from the IGS data center of Wuhan University (<ftp://igs.gnsswhu.cn/pub/gps/products/mgex>, accessed on 26 February 2023).

Since PPP-B2b products are only available in and around the China area, the arc of the single satellite is only about several hours. We cannot use single satellite clock products to calculate the clock time datum. Thus, we propose to calculate the satellite clock time datum by using all satellites. It should be noted that this method also contains the time datum of reference products. Firstly, Figure 1 presents the single-differenced satellite clock series between two products. B2b-gbm, B2b-wum, and gbm-wum represent the single-differenced satellite clock between PPP-B2b and gbm products, between PPP-B2b and wum products, and between gbm and wum products, respectively. As for GPS satellites, the single-differenced satellite clock series of B2b-gbm and B2b-wum show larger noises than that of gbm-wum. According to Equation (6), the single-differenced satellite clock contains the satellite clock error and time datum of two products. Thus, the common jumps of all satellites should be attributed to satellite clock time data, while the others should be attributed to satellite clock errors. As for BDS-3 satellites, all the results show a linear trend in the time series. It should be noted the linear trends in single-differenced satellite clocks are caused by the different processing strategies and will be absorbed into the receiver clock. It can be canceled by a single difference between two receivers and will not affect the accuracy of positioning and time synchronization.

Based on Figure 1 and Equation (7), we can derive the satellite clock time datum series, which are given in Figure 2. It should be noted that constant values are added to the time datum series for comparison. The results show that the GPS satellite clock time datum series of B2b-gbm and B2b-wum is not stable while the time datum series of gbm-wum are quite stable. Thus, the jumps in the GPS satellite clock time datum series of B2b-gbm and B2b-wum are caused by the PPP-B2b product. As for BDS-3, the satellite clock time datum series of B2b-gbm, B2b-wum, and gbm-wum are all quite smooth. However, there are different linear trends in the three results. The variations, which are caused by the different time datums, are less than 6 ns for one day. Among the three series of BDS-3 satellite clock time data, the time datum between PPP-B2b and wum products is the most consistent, and the variation is only about 1.3 ns.

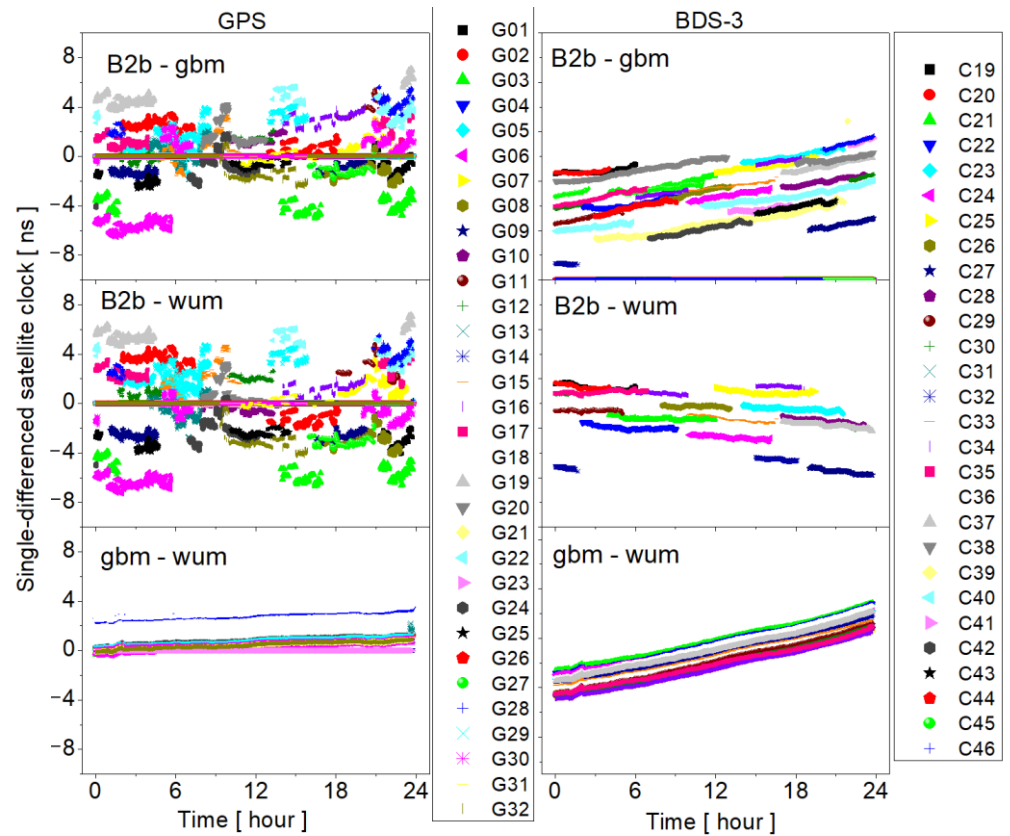


**Figure 1.** Single-differenced satellite clock series between different products in MJDN 59100 (8 September 2020); B2b, gbm, and wum represent products of PPP-B2b, GFZ, and WHU.

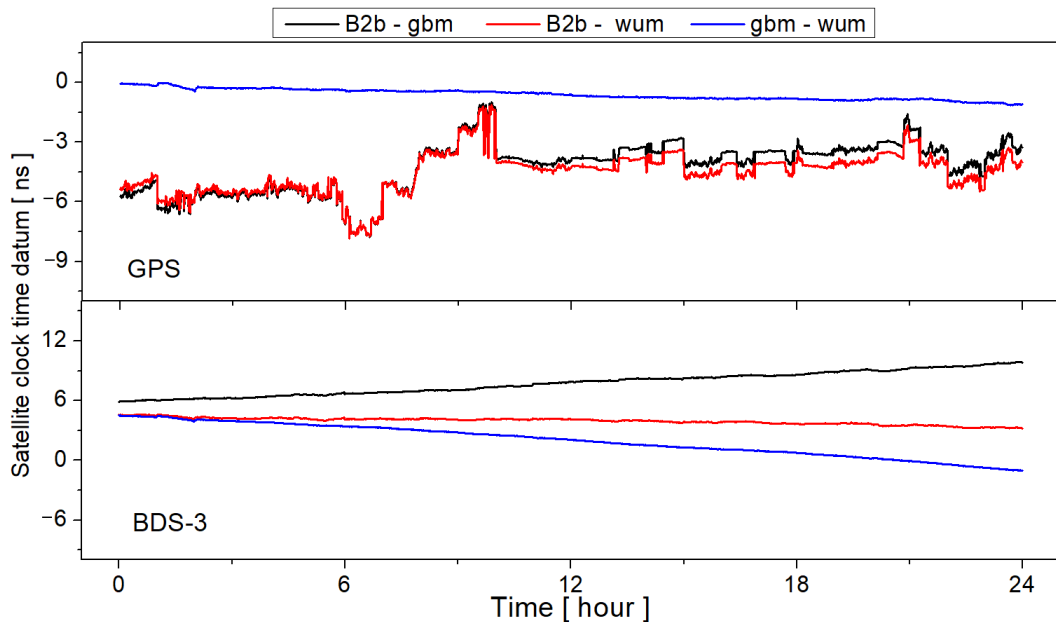


**Figure 2.** Satellite clock time datum between different products in MJDN 59100 (8 September 2020); B2b, gbm, and wum represent products of PPP-B2b, GFZ, and WHU; constant values are added to the time datum series for comparison.

The overlapping Allan deviation (ADEV) can be used to evaluate the stability of the satellite clock time datum [27]. Figure 3 gives the GPS and BDS-3 ADEV according to the

time datum series of B2b-gbm. According to the results, the average ADEVs are about  $8 \times 10^{-12}$  and  $8 \times 10^{-13}$  at 30 s for GPS and BDS-3, respectively. When the average time is  $10^4$  s, the average ADEVs are about  $1 \times 10^{-13}$  and  $2 \times 10^{-14}$  for GPS and BDS-3, respectively. In addition, the ADEV of the GPS satellite clock time datum is more consistent than that of BDS-3 for different weeks, while the time datum of BDS-3 is more stable than that of GPS. Overall, the BDS-3 ADEV of time datum is about one order of magnitude smaller than that of the GPS, which is consistent with the results in Figure 2.

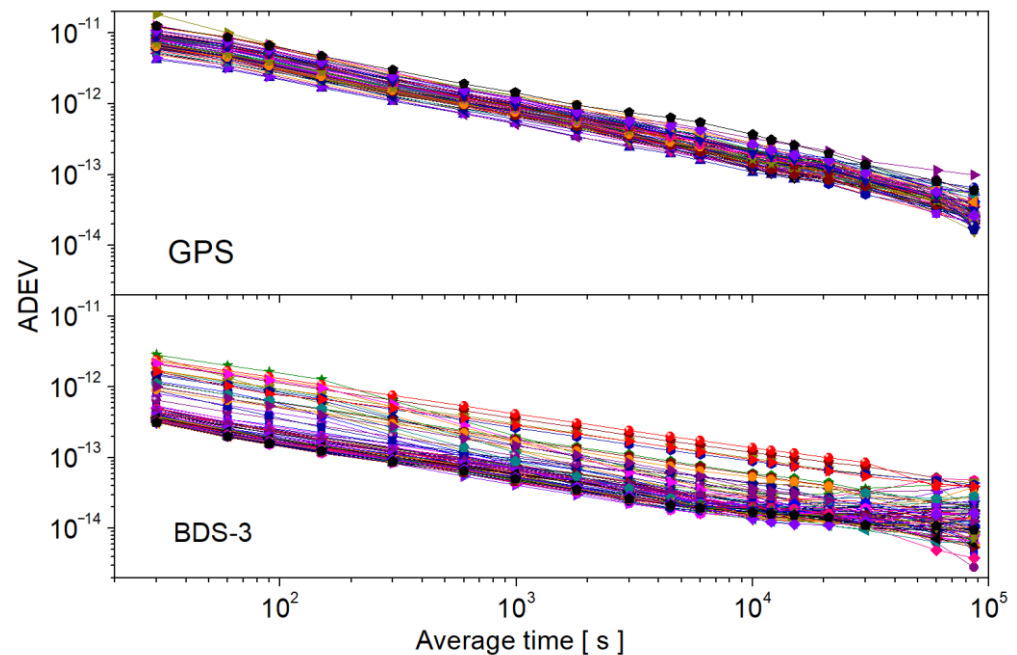


**Figure 3.** Allan deviation of B2b-gbm; each line represents ADEV calculated from one-week product.

In addition to the time datum stability of the satellite clock, product accuracy is also an important factor affecting precise time service. Figure 4 shows the GPS and BDS-3 satellite orbit and clock error series. Since the service region is in and around the China areas, the PPP-B2b products are also not full arc in the day. According to the satellite orbit error series, the satellite orbits of PPP-B2b are predicted products, and there are obvious boundary jumps when the satellite orbits are updated. The maximum boundary jump could reach up to 0.7 m for the GPS G20 satellite from 1.18 m to 0.48 m in the along component. Among the three directions of the satellite orbit, the radial accuracy is the best, and the tangential accuracy is the worst. In addition, the accuracy of satellite orbit after 9 o'clock is better than those before 9 o'clock on this day, especially for along and cross components. This may be related to the data integrity of observations in real-time processing. As for the satellite clock, large biases are also observed, which is similar to the results of [15].

Figure 5 presents the satellite orbit time series of PPP-B2b products. According to Figure 5, the accuracy of the satellite orbit is quite stable for PPP-B2b products, except for some outliers of GPS satellites, especially in along and cross directions. As for radial direction, the RMSE series of BDS-3 satellite is more stable than that of the GPS satellite. Overall, the satellite orbit accuracy of GPS is slightly worse than that of BDS-3 satellites, which may be attributed to the use of inter-satellite link data. Limited to observations used for real-time orbit determination, the satellite orbit accuracy of the PPP-B2b product is much worse than that of current real-time space state representation (SSR) products from IGS Analysis Centers [28], which may greatly improve if more global stations are added to satellite orbit estimation in the future.

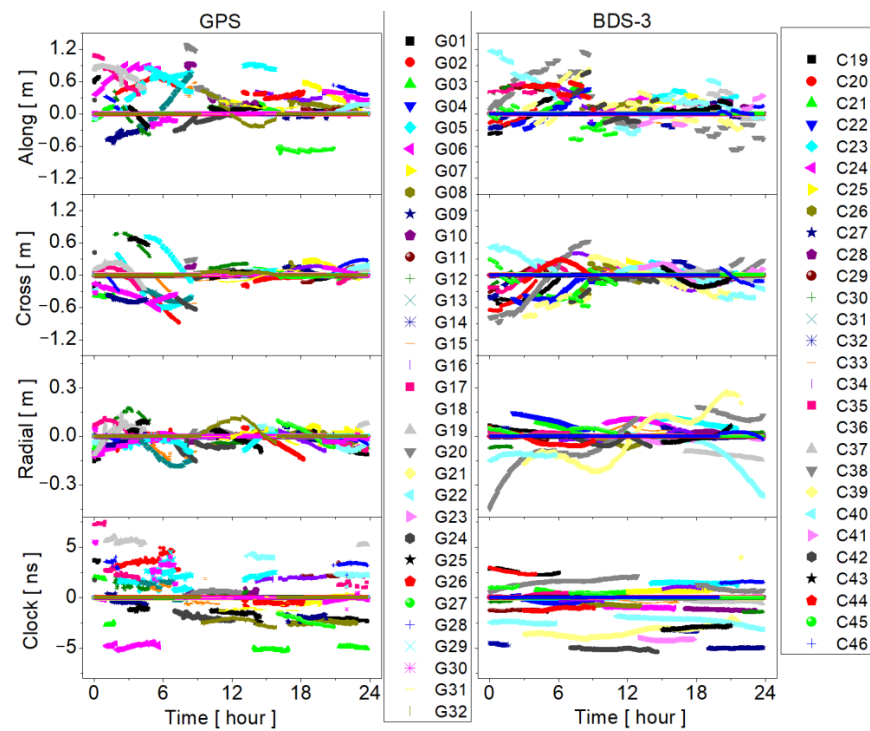


**Figure 4.** Satellite orbit and clock error time series of PPP-B2b products in MJDN 59100 (9 September 82020).

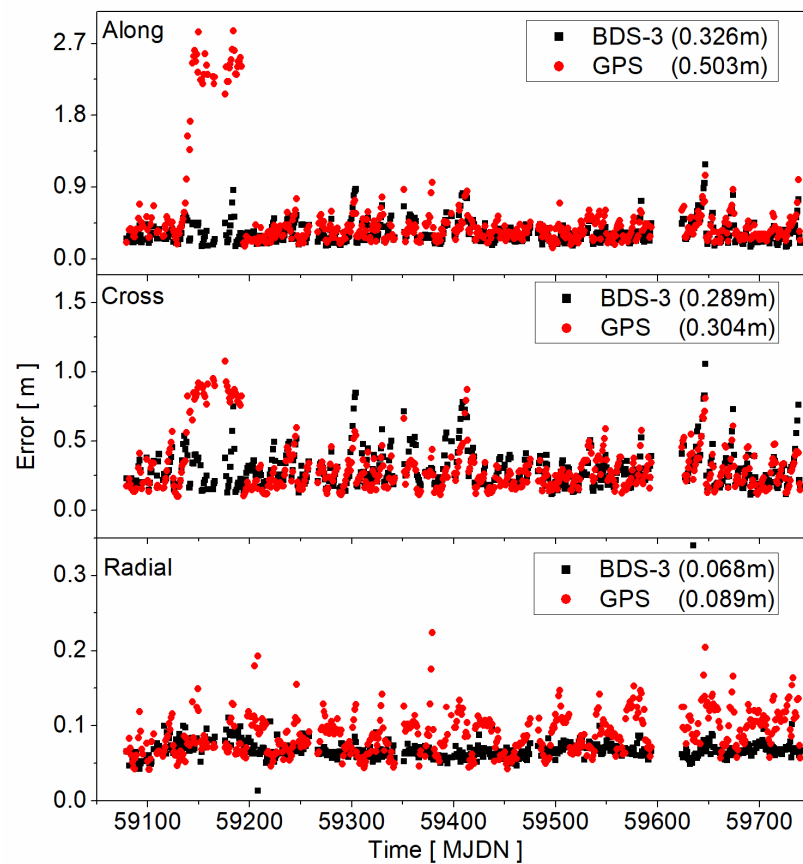


**Figure 5.** Time series of satellite orbit error for PPP-B2b products; Black squares and red cycles represent BDS-3 and GPS, respectively; top, middle, and bottom panels are the RMS of satellite orbit in Along, Cross, and Radial directions, respectively.

Figure 6 presents the time series of the satellite clock RMSE, STD. In addition, we also give the STD of SISRE since the satellite orbit and clock are coupled. The average satellite clock RMSE is 1.97 ns and 2.45 ns for BDS-3 and GPS, respectively. Overall, the satellite clock accuracy of the BDS-3 satellite is better than that of the GPS satellite for both RMSE and STD. Although the large RMSE of the satellite clock will not greatly affect the accuracy of PPP after convergence, it will slow down the convergence speed of PPP. As for the satellite clock and SISRE STD, the accuracy of BDS-3 is also better than that of the GPS. Among them, the average value of SISRE STD is only 0.13 ns for BDS-3 satellites, while it is 0.22 ns for GPS satellites. Generally, a smaller SISRE STD means a more stable PPP performance. In other words, it means the performance of BDS-3 PPP will be better than that of GPS PPP based on PPP-B2b products if the observation qualities of GPS and BDS-3 are at the same level. Finally, according to Figures 5 and 6, the satellite orbit and clock accuracy of PPP-B2b products have been quite stable over these 557 days.

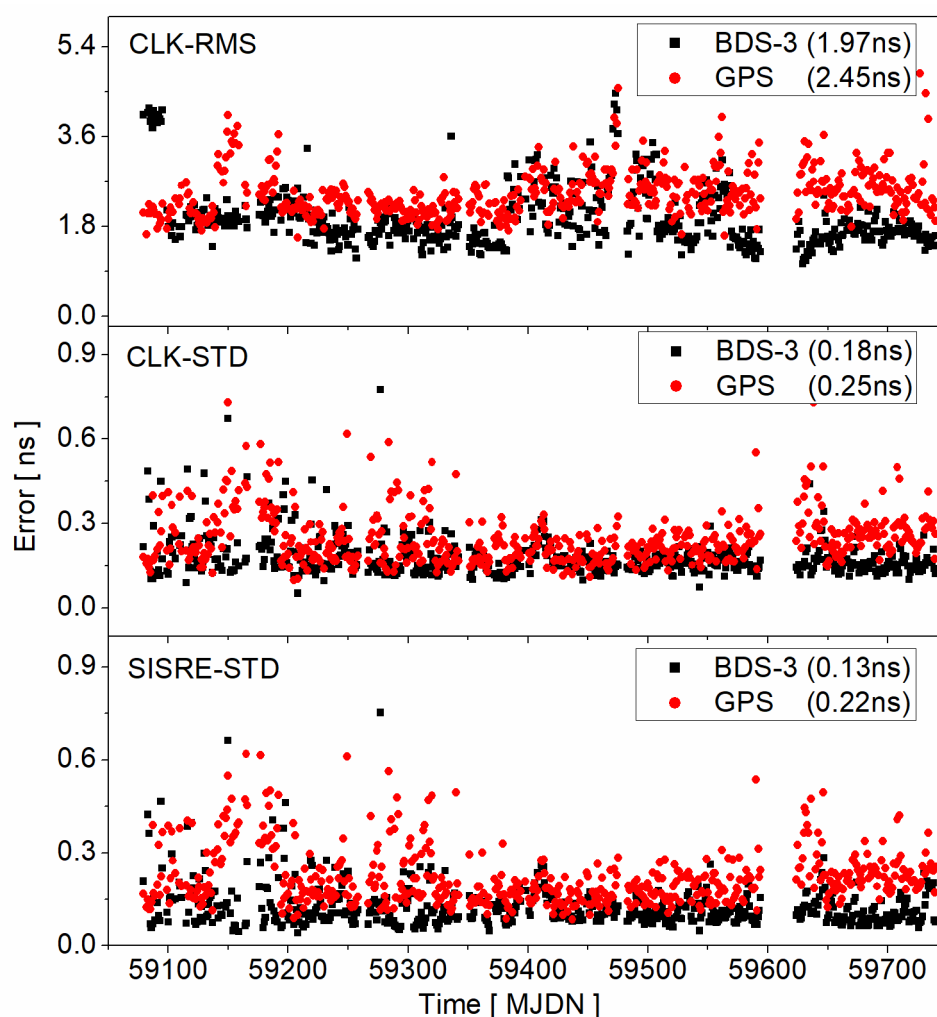


**Figure 6.** Time series of satellite clock error and SISRE for PPP-B2b products; Black squares and red cycles represent BDS-3 and GPS, respectively; top, middle, and bottom panels are satellite clock RMS, satellite clock STD, and SISRE STD, respectively.

## 4. Experiment

### 4.1. Data and Strategy

In this section, the data and strategy used for timing and time synchronization are presented. To explore the performance of BDS-3 and GPS timing and time synchronization based on PPP-B2b products, 8 stations located in and around China are adopted in this paper. Figure 7 is the station distribution of these 8 stations. As for time synchronization

validation, 10 baselines are formed based on these 8 stations from 13 km to 4494 km, and the detailed information is given in Table 1.

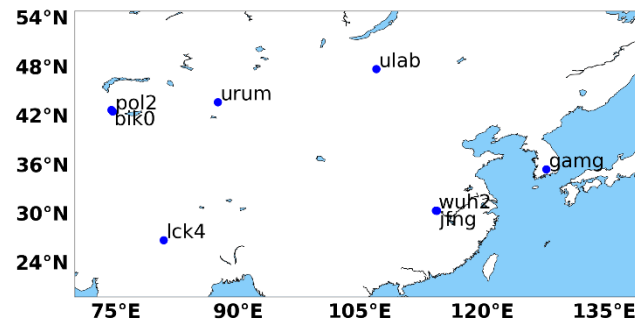


Figure 7. Station distribution used in this paper.

Table 1. Baseline information.

Number	Station Name	Length (km)
BL01	jfng—wuh2	13
BL02	bik0—pol2	23
BL03	pol2—urum	1053
BL04	gamg—jfng	1370
BL05	lck4—pol2	1833
BL06	gamg—ulab	2184
BL07	jfng—urum	2766
BL08	lck4—ulab	3213
BL09	gamg—urum	3493
BL10	gamg—lck4	4494

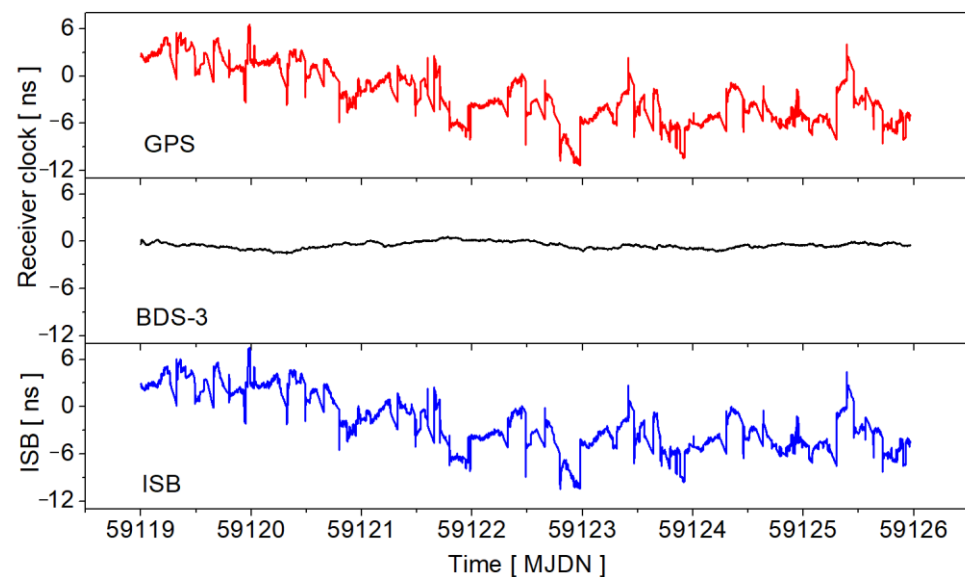
In this paper, the IF combination is used for receiver clock estimation. The specific PPP processing strategies are listed in Table 2. We use a PPP float solution since PPP-B2b products do not contain phase bias currently. In addition, the receiver clocks are estimated as white noise for each satellite system. Since the observation interval is 30 s, the processing interval of timing and time synchronization is 30 s in the experiments.

Table 2. PPP processing strategy.

Items	Strategy
Satellite orbit and clock	Fixed by broadcast ephemeris and PPP-B2b
Troposphere delay	Corrected by GPT2 model and estimated zenith troposphere with GMF mapping function [29]
Ionosphere delay	Eliminate 1st order ionosphere delay by IF combination
Receiver clock	Estimated as white noise for each satellite system
Ambiguity	Float solution and estimated as a constant value for each arc
Receiver coordinate	Estimated as static parameters
Observations	GPS: L1/L2
Cutoff elevation	BDS-3: B1I/B3I 7°
Weighting ( $p$ )	$\begin{cases} p = 1, & ele > 30^\circ \\ p = \sin(ele) & ele \leq 30^\circ \end{cases}$ , applied for code/phase
Satellite antenna phase center	BDS-3 PCO from official website; GPS PCOs and PCVs from IGS MGEX
Phase wind-up	Corrected with [30]
Processing interval	30 s

#### 4.2. PPP One-Way Timing

In this section, lck4 is selected for PPP timing evaluation since it is equipped with a high-performance atomic clock. Only one-week results are given limited to data. Figure 8 gives the receiver clock and inter-system bias (ISB) series of station lck4 in a week (from MJDN 59119 to 59126). According to the results, the GPS receiver clock shows large noises and jumps in its series. However, the BDS-3 receiver clock series are much more stable than that of the GPS. The variations of GPS and BDS-3 receiver clocks are about 18 ns and 2 ns in a week, respectively. The estimated receiver clock mainly consists of the true receiver clock, hardware delay, and time datum of products. On one hand, GPS and BDS-3 of station lck4 share the same true receiver clock. On the other hand, the hardware delay has generally been stable over a long period [31]. Thus, the difference between the estimated GPS and BDS-3 receiver clocks is caused by the different time datum in PPP-B2b products, which is also validated in Figure 2. As a result, the ISB between GPS and BDS-3 also jumps in its series, which means that the ISB parameters cannot be estimated as constant values if users use PPP-B2b products.



**Figure 8.** Receiver clock and ISB series of station lck4, the top, middle, and bottom panels represent GPS receiver clock, BDS-3 receiver clock, and ISB, respectively.

Figure 9 presents the overlapping ADEV of station lck4 receiver clock estimated by GPS and BDS-3 observations. Similarly, the stability of the GPS receiver clock is worse than that of BDS-3. Generally, the BDS-3 receiver clock is an order of magnitude more stable than that of GPS. For example, the ADEVs are about  $2.78 \times 10^{-13}$  and  $2.90 \times 10^{-14}$  for GPS and BDS-3 at  $10^4$  s. Overall, the stability of BDS-3 one-way PPP timing with PPP-B2b products is at the same level as that of IGS analysis center real-time products [27]. However, the stability of GPS one-way PPP timing with PPP-B2b is much worse and needs further improvement. Since the average SISRE-STD of GPS is as high as 0.22 ns, the main reason should be attributed to the poor stability of the satellite clock time datum in the PPP-B2b product.

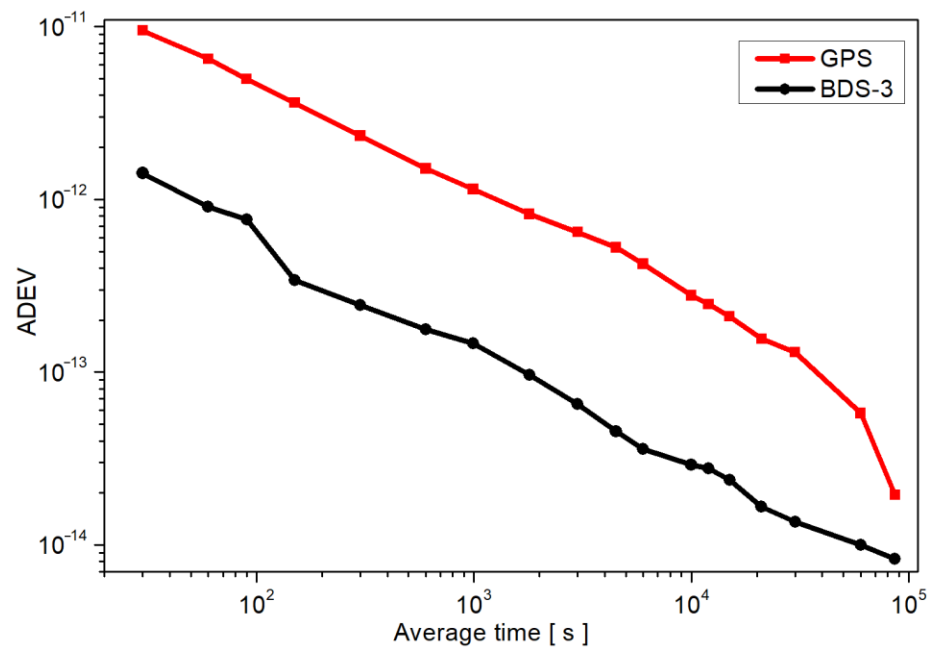


Figure 9. Allan deviation of lck4 receiver clock series from PPP one-way timing from MJDN 59119 to 59126, with products of PPP-B2b.

### 4.3. PPP Time Synchronization

In this section, we mainly focus on the performance of PPP time synchronization based on PPP-B2b products. Since not all stations are equipped with high-performance atomic, the receiver clocks estimated based on GFZ products are treated as reference values. Figure 10 presents the single-differenced receiver clock series of 8 stations in MJDN 59511. There are jumps in single-differenced receiver clock series for GPS. Moreover, the jumps are almost the same for all stations, which should be caused by the GPS satellite clock time datum of PPP-B2b products. However, as for BDS-3 receiver clocks, the series is smoother than that of the GPS, and there is about a 1 ns bias of the receiver clock between the bik0 station and other stations.

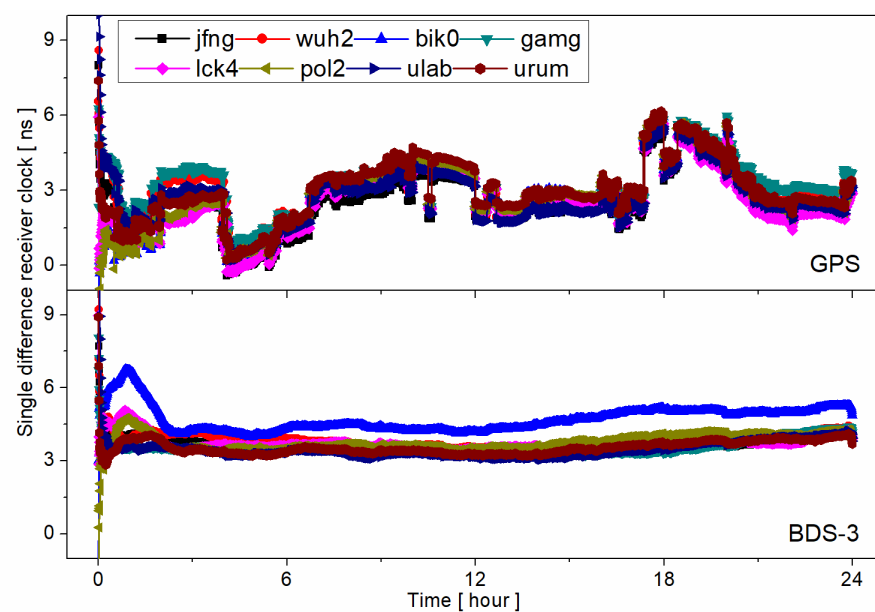
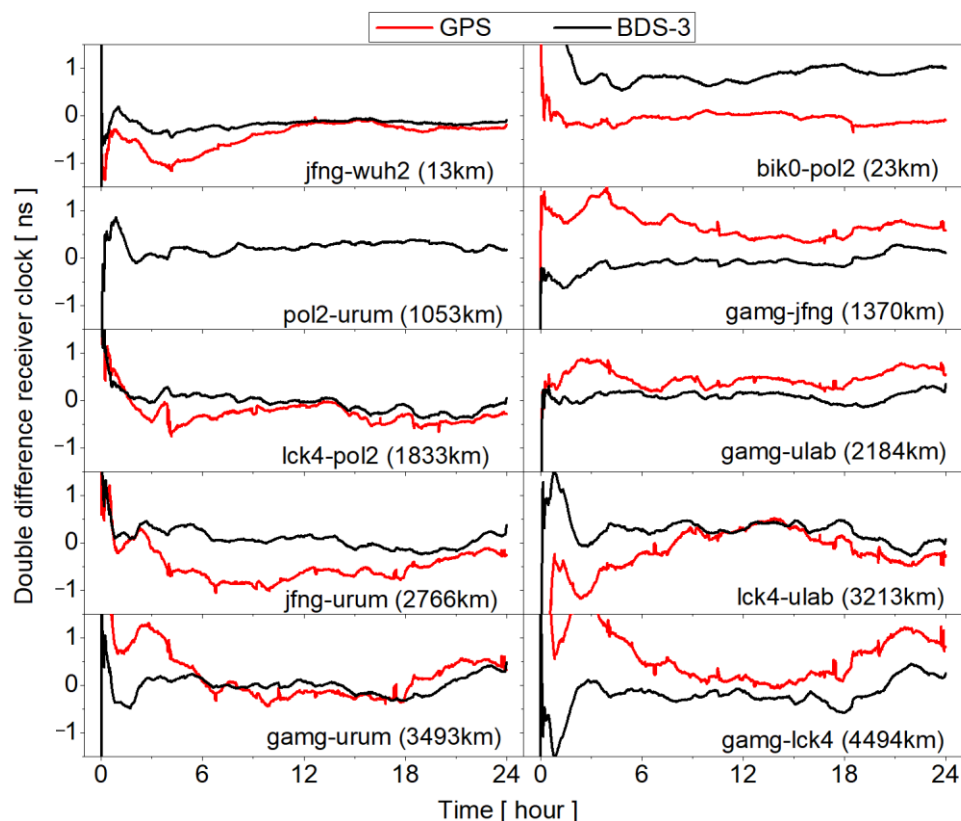


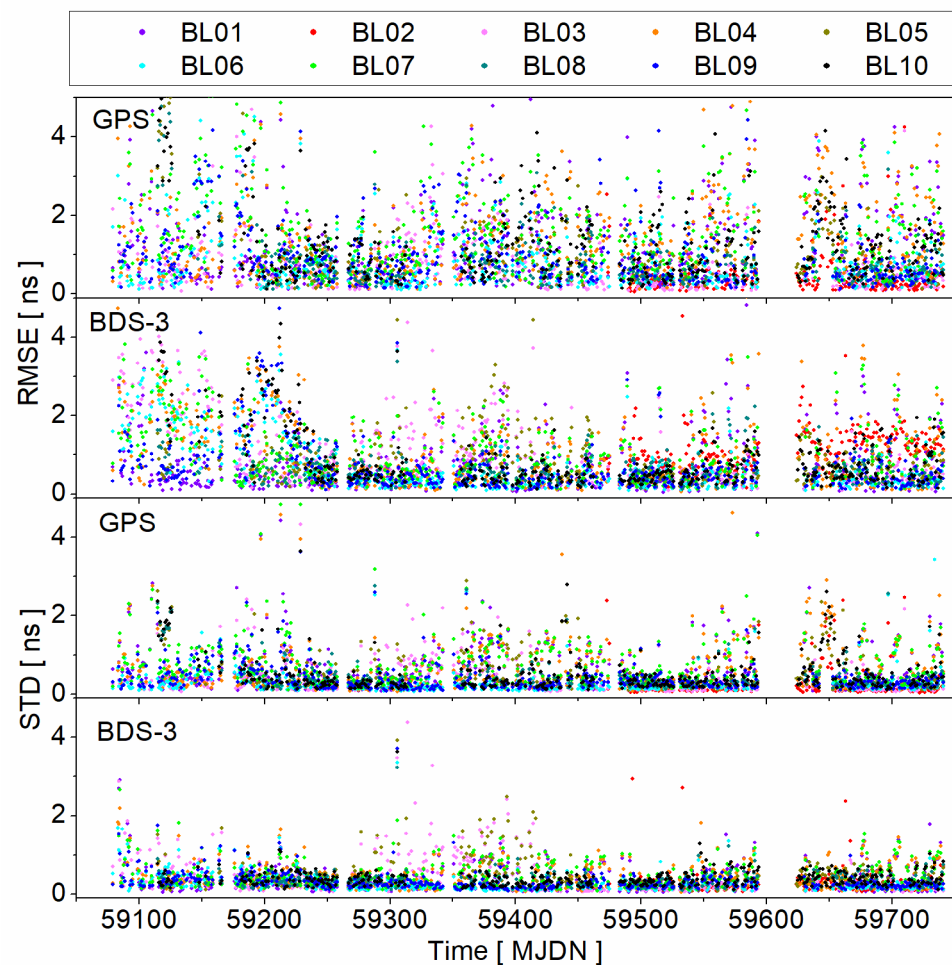
Figure 10. Single-differenced receiver clock series in MJDN 59511; the top and bottom panels are GPS and BDS-3 receiver clocks, respectively.

Figure 11 shows the GPS and BDS-3 time synchronization series of 10 baselines from 13 km to 4494 km. In these experiments, the receiver clock needs several hours to converge at the initial phase. Among the 10 baselines, although the baseline of bik0-pol2 is only 23 km, the BDS-3 time synchronization series still show about a 1 ns systematic bias. As for other baselines, the biases of BDS-3 time synchronization are all less than those of bik0-pol2. According to Figure 10, the 1 ns bias is caused by station bik0. This may be the result of the combined influence of observation quality and different available satellites between PPP-B2b and gbm products.



**Figure 11.** Double-differenced receiver clock series in MJDN 59511; the black and red lines represent GPS and BDS-3 receiver clocks, respectively.

For the long-term evaluation, Figure 12 presents the time synchronization results of 557 day from 10 baselines. Since there is an obvious convergence time for both the GPS and BDS-3 receiver clock estimation, the initial two-hour receiver clocks are not involved in RMSE and STD calculation. According to Figure 12, the RMSEs of GPS and BDS-3 time synchronization with PPP-B2b products are mostly within 5 ns, while the STDs of GPS and BDS-3 time synchronization are mostly within 2 ns. Additionally, the accuracy of GPS time synchronization is worse than that of BDS-3 for both RMSE and STD. This is consistent with the assessment of SISRE STD in Figure 6. Similar to the results in Figure 11, baseline length is not the most important factor that affects the precision of time synchronization. For example, the STDs of BL03, BL05, and BL07 are significantly larger than that of BL09 and BL10 from MJDN 59300 to 59400.



**Figure 12.** RMSE and STD series of time synchronization from 10 baselines; the 1st and 2nd panels represent RMSE of time synchronization for GPS and BDS-3, respectively; the 3rd and 4th panels represent STD of time synchronization for GPS and BDS-3, respectively.

Based on the results of Figure 12, Table 3 summarizes the average RMSEs and STDs of time synchronization from 10 baselines. The results demonstrate the average RMSEs of GPS time synchronization are from 0.46 ns to 1.58 ns and from 0.66 ns to 1.19 ns for BDS-3. As for STDs, the average STDs are from 0.27 ns to 0.74 ns and from 0.27 ns to 0.47 ns for GPS and BDS-3, respectively. In addition, there is no relationship between baseline length and time synchronization precision, which means the baseline length is not the most important factor that affects the precision of time synchronization in this experiment.

**Table 3.** Average RMSEs of time synchronization from 10 baselines.

Number	Length (km)	RMSE (ns)		STD (ns)	
		GPS	BDS-3	GPS	BDS-3
BL01	13	1.24	0.73	0.64	0.40
BL02	23	0.46	1.19	0.27	0.27
BL03	1053	0.80	1.01	0.40	0.44
BL04	1370	1.42	1.04	0.68	0.46
BL05	1833	1.03	0.77	0.52	0.47
BL06	2184	0.90	0.74	0.30	0.28
BL07	2766	1.58	1.02	0.74	0.47
BL08	3213	0.94	0.66	0.44	0.35
BL09	3493	1.00	0.72	0.41	0.32
BL10	4494	1.24	0.87	0.50	0.39

## 5. Conclusions and Outlook

PPP technology is widely used for time service, which needs high-precision satellite orbit and clock products. The BDS-3 PPP-B2b signal can provide real-time high-precision satellite orbit and clock products, which can meet the demands of PPP services for China and its surrounding areas. In this paper, we focus on the evaluation of PPP-B2b products. PPP-B2b products from MJDN 59079 (18 August 2020) to 59740 (11 June 2022), which are collected by our own receivers, are adopted for time datum stability and accuracy evaluation. The PPP-B2b corrections are converted to precise satellite orbit and clock products by matching the IOD of broadcast ephemeris and IODN of PPP-B2b corrections.

Firstly, PPP-B2b products are evaluated with reference to satellite orbit and clock products from IGS ACs. The results show that there are large jumps in the GPS satellite clock time datum series. The ADEV is about  $1 \times 10^{-13}$  @ $10^4$  s. However, the BDS-3 satellite clock time datum is more stable than that of GPS. The ADEV is about  $2 \times 10^{-14}$  @ $10^4$  s. In addition, the satellite orbit accuracy of GPS and BDS-3 satellites is generally at the same level, which is much worse than that of current real-time IGS SSR products. In addition, the satellite clock RMSE and STD of the BDS-3 satellite are better than those of the GPS satellite. As for SISRE STD, the average values are 0.13 ns and 0.22 ns for BDS-3 and GPS, respectively. The satellite orbit and clock accuracy of PPP-B2b products are stable according to their series.

Then, observations from the MGEX network are used for PPP-B2b product evaluation by using PPP one-way timing and time synchronization. As for PPP one-way timing, station lck4 is equipped with high-performance atomic. There are jumps in the GPS receiver clock series, which also validates that the time datum stability of the GPS satellite clock is worse than that of the BDS-3 satellite clock. Generally, the BDS-3 receiver clock is an order of magnitude more stable than that of GPS. As a result, the time datum between GPS and BDS-3 jumps in its series, which will be absorbed into the ISB parameter. This indicates that the ISB parameters cannot be estimated as constant values if users use PPP-B2b products. As for PPP time synchronization, 10 baselines from 13 km to 4494 km are formed. The results demonstrate that the average RMSEs of GPS time synchronization are from 0.46 ns to 1.58 ns and from 0.66 ns to 1.19 ns for BDS-3. As for STDs, the average STDs are from 0.27 ns to 0.74 ns and from 0.27 ns to 0.47 ns for GPS and BDS-3, respectively.

Overall, the 557-day results show that the time datum stability and accuracy of PPP-B2b products are stable. In addition, the time synchronization STDs of 10 baselines during the 557 days are mostly within 2 ns, and the average values are all better than 1 ns.

**Author Contributions:** Conceptualization, Q.H., L.L.; methodology, L.C., X.G.; validation, Q.G., D.Z.; writing—original draft preparation, Q.H.; writing—review and editing, Q.H., L.C., Y.L., X.G.; visualization, Q.H.; funding acquisition, X.G. All authors have read and agreed to the published version of the manuscript.

**Funding:** This research was funded by the National Natural Science Foundation of China (42274023) and Young Elite Scientists Sponsorship Program by CAST (No. YESS20210184).

**Data Availability Statement:** The data presented in this study are available on request from the corresponding author. The data are not publicly available due to the company policy restrictions.

**Acknowledgments:** The authors show great gratitude to IGS for providing data.

**Conflicts of Interest:** The authors declare no conflict of interest.

## References

1. Montenbruck, O.; Steigenberger, P.; Prange, L.; Deng, Z.; Zhao, Q.; Perosanz, F.; Schaer, S. The Multi-GNSS Experiment (MGEX) of the International GNSS Service (IGS)—achievements, prospects and challenges. *Adv. Space Res.* **2017**, *59*, 1671–1697. [[CrossRef](#)]
2. Zumberge, J.F.; Heflin, M.B.; Jefferson, D.C.; Watkins, M.M.; Webb, F.H. Precise point positioning for the efficient and robust analysis of GPS data from large networks. *J. Geophys. Res. Solid Earth* **1997**, *102*, 5005–5017. [[CrossRef](#)]
3. Li, X.; Huang, J.; Li, X.; Shen, Z.; Han, J.; Li, L.; Wang, B. Review of PPP-RTK: Achievements, challenges, and opportunities. *Satell. Navig.* **2022**, *3*, 28. [[CrossRef](#)]

4. Geng, J.; Guo, J.; Meng, X.; Gao, K. Speeding up PPP ambiguity resolution using triple-frequency GPS/BeiDou/Galileo/QZSS data. *J. Geodesy* **2020**, *94*, 6. [[CrossRef](#)]
5. Zhang, P.; Tu, R.; Han, J.; Gao, Y.; Zhang, R.; Lu, X. Characterization of biases between BDS-3 and BDS-2, GPS, Galileo and GLONASS observations and their effect on precise time and frequency transfer. *Meas. Sci. Technol.* **2021**, *32*, 035006. [[CrossRef](#)]
6. Cai, H.; Meng, Y.; Geng, C.; Gao, W.; Zhang, T.; Li, G.; Shao, B.; Xin, J.; Lu, J.; Mao, Y.; et al. BDS-3 performance assessment: PNT, SBAS, PPP, SMC and SAR. *Acta Geod. Cartogr. Sin.* **2021**, *50*, 427–435.
7. Yang, Y.; Gao, W.; Guo, S.; Mao, Y.; Yang, Y. Introduction to BeiDou-3 navigation satellite system. *Navigation* **2019**, *66*, 7–18. [[CrossRef](#)]
8. Liu, C.; Gao, W.; Liu, T.; Wang, D.; Yao, Z.; Gao, Y.; Nie, X.; Wang, W.; Li, D.; Zhang, W.; et al. Design and implementation of a BDS precise point positioning service. *Navigation* **2020**, *67*, 875–891. [[CrossRef](#)]
9. Tang, C.; Hu, X.; Chen, J.; Liu, L.; Zhou, S.; Guo, R.; Li, X.; He, F.; Liu, J.; Yang, J. Orbit determination, clock estimation and performance evaluation of BDS-3 PPP-B2b service. *J. Geodesy* **2022**, *96*, 60. [[CrossRef](#)]
10. Yang, Y.; Ding, Q.; Gao, W.; Li, J.; Xu, Y.; Sun, B. Principle and performance of BDSBAS and PPP-B2b of BDS-3. *Satell. Navig.* **2022**, *3*, 5. [[CrossRef](#)]
11. Xu, Y.; Yang, Y.; Li, J. Performance evaluation of BDS-3 PPP-B2b precise point positioning service. *GPS Solutions* **2021**, *25*, 142. [[CrossRef](#)]
12. Gong, X.; Lou, Y.; Zheng, F.; Gu, S.; Shi, C.; Liu, J.; Jing, G. Evaluation and calibration of BeiDou receiver-related pseudorange biases. *GPS Solutions* **2018**, *22*, 98. [[CrossRef](#)]
13. Gong, X.; Gu, S.; Zheng, F.; Wu, Q.; Liu, S.; Lou, Y. Improving GPS and Galileo precise data processing based on calibration of signal distortion biases. *Measurement* **2021**, *174*, 108981. [[CrossRef](#)]
14. Gong, X.; Zheng, F.; Gu, S.; Zhang, Z.; Lou, Y. The long-term characteristics of GNSS signal distortion biases and their empirical corrections. *GPS Solutions* **2022**, *26*, 52. [[CrossRef](#)]
15. Tao, J.; Liu, J.; Hu, Z.; Zhao, Q.; Chen, G.; Ju, B. Initial Assessment of the BDS-3 PPP-B2b RTS compared with the CNES RTS. *GPS Solutions* **2021**, *25*, 131. [[CrossRef](#)]
16. Liu, Y.; Yang, C.; Zhang, M. Comprehensive Analyses of PPP-B2b Performance in China and Surrounding Areas. *Remote Sens.* **2022**, *14*, 643. [[CrossRef](#)]
17. Ren, Z.; Gong, H.; Peng, J.; Tang, C.; Huang, X.; Sun, G. Performance assessment of real-time precise point positioning using BDS PPP-B2b service signal. *Adv. Space Res.* **2021**, *68*, 3242–3254. [[CrossRef](#)]
18. Zhang, W.; Lou, Y.; Song, W.; Sun, W.; Zou, X.; Gong, X. Initial assessment of BDS-3 precise point positioning service on GEO B2b signal. *Adv. Space Res.* **2021**, *69*, 690–700. [[CrossRef](#)]
19. Song, W.; Zhao, X.; Lou, Y.; Sun, W.; Zhao, Z. Performance Evaluation of BDS-3 PPP-B2b Service. *Geomat. Inf. Sci. Wuhan Univ.* **2021**. [[CrossRef](#)]
20. Zhu, E.; Guo, H.; Li, J.; Xiao, H.; Duan, R. Performance Analysis of Real-Time PPP Based on BDS-3 PPP-B2b Service. *J. Geod. Geodyn.* **2022**, *42*, 616–621.
21. He, C.; Gu, S.; Liu, C.; Gao, W.; Zheng, F.; Gong, X.; Li, W. Simulation research on PPP-RTK performance based on BDS GEO satellite. *Meas. Sci. Technol.* **2022**, *33*, 065025. [[CrossRef](#)]
22. Yang, H.; Ji, S.; Weng, D.; Wang, Z.; He, K.; Chen, W. Assessment of the Feasibility of PPP-B2b Service for Real-Time Coseismic Displacement Retrieval. *Remote Sens.* **2022**, *13*, 5011. [[CrossRef](#)]
23. Xu, X.; Nie, Z.; Wang, Z.; Wang, B.; Du, Q. Performance Assessment of BDS-3 PPP-B2b/INS Loosely Coupled Integration. *Remote Sens.* **2022**, *14*, 2957. [[CrossRef](#)]
24. Geng, T.; Li, Z.; Xie, X.; Liu, W.; Li, Y.; Zhao, Q. Real-time ocean precise point positioning with BDS-3 service signal PPP-B2b. *Measurement* **2022**, *203*, 111911. [[CrossRef](#)]
25. Lu, X.; Chen, L.; Shen, N.; Wang, L.; Jiao, Z.; Chen, R. Decoding PPP Corrections From BDS B2b Signals Using a Software-Defined Receiver: An Initial Performance Evaluation. *IEEE Sensors J.* **2021**, *21*, 7871–7883. [[CrossRef](#)]
26. Zhang, R.; He, Z.; Ma, L.; Xiao, G.; Guang, W.; Ge, Y.; Zhang, X.; Zhang, J.; Tang, J.; Li, X. Analysis of BDS-3 PPP-B2b Positioning and Time Transfer Service. *Remote Sens.* **2022**, *14*, 2769. [[CrossRef](#)]
27. Guo, W.; Zuo, H.; Mao, F.; Chen, J.; Gong, X.; Gu, S.; Liu, J. On the satellite clock datum stability of RT-PPP product and its application in one-way timing and time synchronization. *J. Geodesy* **2022**, *96*, 52. [[CrossRef](#)]
28. Li, B.; Ge, H.; Bu, Y.; Zheng, Y.; Yuan, L. Comprehensive assessment of real-time precise products from IGS analysis centers. *Satell. Navig.* **2022**, *3*, 12. [[CrossRef](#)]
29. Boehm, J.; Niell, A.; Tregoning, P.; Schuh, H. Global Mapping Function (GMF): A new empirical mapping function based on numerical weather model data. *Geophys. Res. Lett.* **2006**, *33*, 199–208. [[CrossRef](#)]
30. Wu, J.; Wu, S.; Hajj, G.; Bertiger, W.; Lichten, S. Effects of antenna orientation on GPS carrier phase. *Manuscr. Geod.* **1993**, *18*, 91–98.
31. Peng, Y.; Dai, X.; Lou, Y.; Gong, X.; Zheng, F. BDS-2 and BDS-3 combined precise orbit determination with hybrid ambiguity resolution. *Measurement* **2022**, *188*, 110593. [[CrossRef](#)]

**Disclaimer/Publisher’s Note:** The statements, opinions and data contained in all publications are solely those of the individual author(s) and contributor(s) and not of MDPI and/or the editor(s). MDPI and/or the editor(s) disclaim responsibility for any injury to people or property resulting from any ideas, methods, instructions or products referred to in the content.